
Figures and figure supplements

Dermomyotome-derived endothelial cells migrate to the dorsal aorta to support hematopoietic stem cell emergence

Pankaj Sahai-Hernandez, Claire Pouget and Shai Eyal et al.

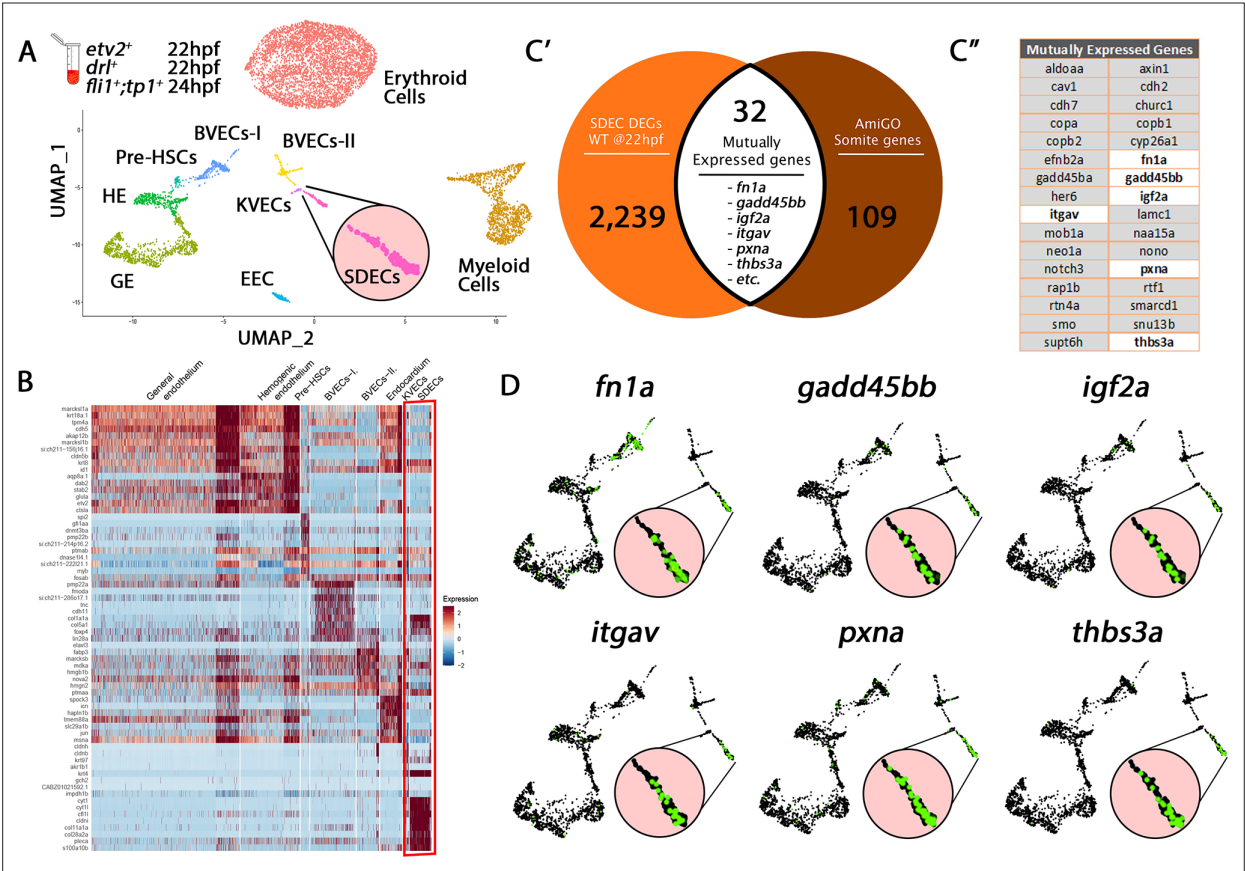


Figure 1. Cell-type-specific endothelial cell markers highlight cellular diversity within the vasculature. **(A)** Uniform manifold approximation projection (UMAP) plots of scRNA-seq data of total endothelial lineage cells collected from *TgBAC(etv2:Kaede)^{ci6}*, *Tg(fli1:DsRed)^{um13}*, *Tg(tp1:GFP)^{um14}*, and *Tg(drl:H2B-dendra)* embryos at 22–24 hpf. Clusters were named according to their gene expression: Erythroid, Lymphoid, General Endothelium (GE), Hemogenic Endothelium (HE), Pre-HSCs, Brain Vascular Endothelial Cells (BVECs-I and BVECs-II), Kidney Vascular Endothelial cells (KVECs), Endocardial Endothelial Cells (EECs), and somite-derived endothelial cells (SDECs). Color-coded marker gene expression levels are shown on corresponding clusters. A pink circle highlights the SDEC cluster. **(B)** Expression heatmap of 22–24 hpf single-cell transcriptome shows the top predicted differentially expressed marker genes across the different clusters. A red box highlights the SDEC cluster. **(C',C'')** A list of somite-annotated genes was curated from the AmiGo annotation database and compared with the SDEC transcriptome. 32 genes were commonly expressed. Interestingly, several of these 32 genes were enriched within the SDEC cluster (**C''**; white boxed genes, **D**; enlarged circles).

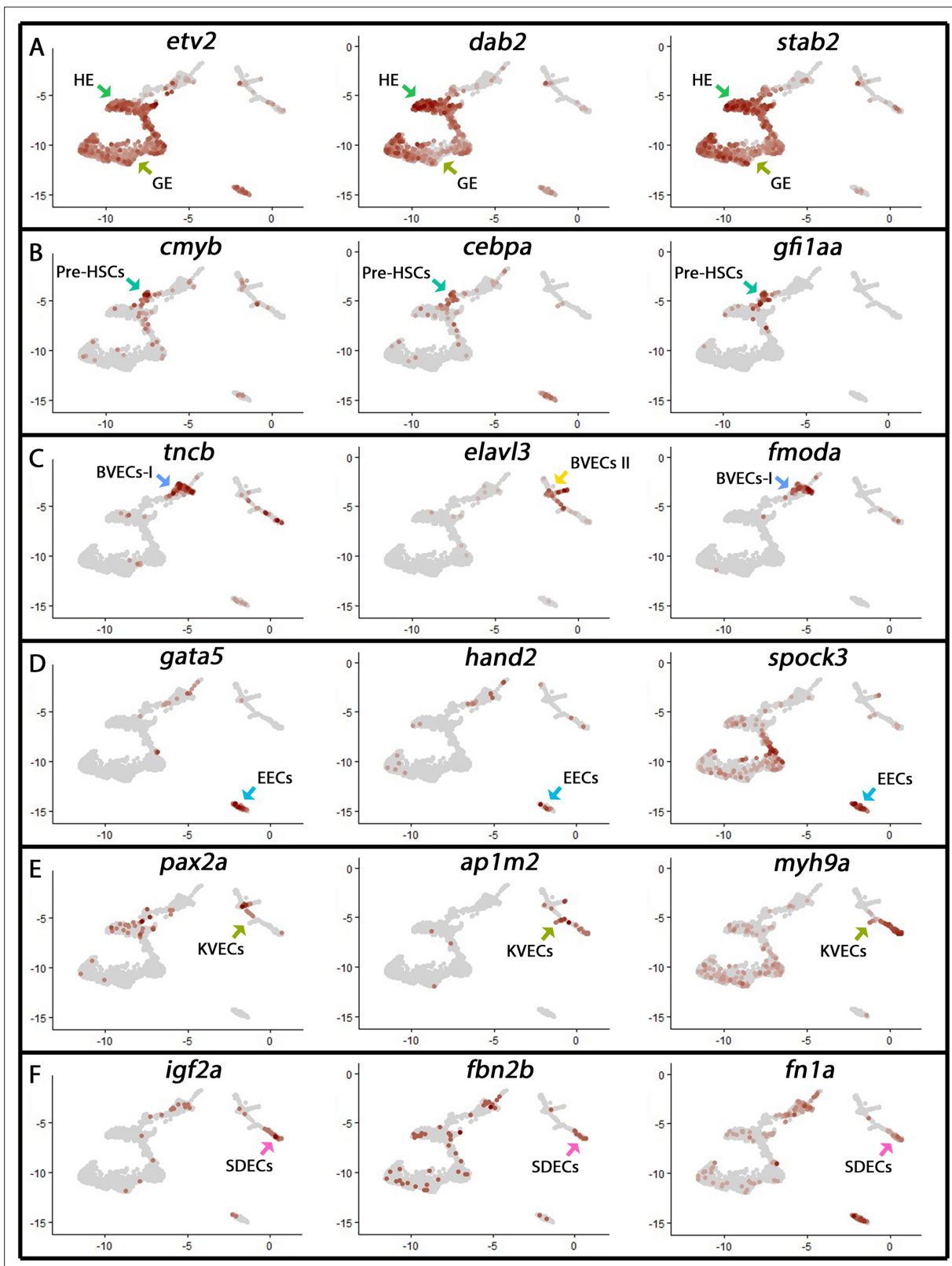


Figure 1—figure supplement 1. Cluster identity was assigned based on known marker genes. (A–F) Following unsupervised clustering of single-cell transcriptomes, cluster identity was given based on known marker genes within established tissue lineages. Selected marker genes and the eight distinct endothelial cell clusters are shown (arrows, color-coded by their original cluster color in **Figure 1A**).

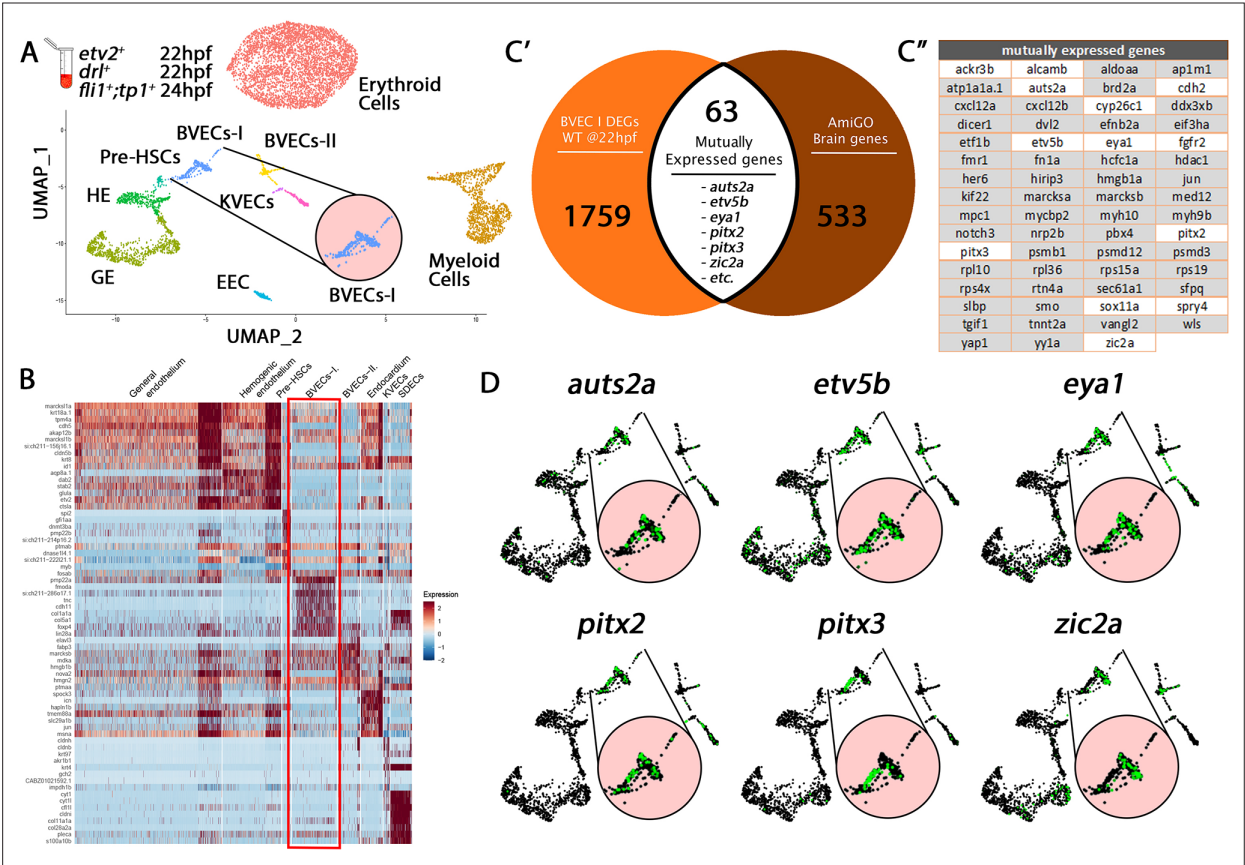


Figure 1—figure supplement 2. Comparison of BVECs-I cluster genes to brain annotated genes validates cluster origin. **(A)** Uniform manifold approximation projection (UMAP) plots of scRNA-seq data of total endothelial lineage cells collected from *TgBAC(etv2:Kaede)^{ci6}*, *Tg(fli1:DsRed)^{um13}*, *Tg(tp1:GFP)^{um14}*, and *Tg(drl:H2B-dendra)* embryos at 22–24 hpf. Clusters were named according to their gene expression: Erythroid, Lymphoid, General Endothelium (GE), Hemogenic Endothelium (HE), Pre-HSCs, Brain Vascular Endothelial Cells (BVECs-I and BVECs-II), Kidney Vascular Endothelial cells (KVECs), Endocardial Endothelial Cells (EECs), and somite-derived endothelial cells (SDECs). Color-coded marker gene expression levels are shown on corresponding clusters. A pink circle highlights the BVECs-I cluster. **(B)** Expression heatmap of 22–24 hpf single-cell transcriptome showing the top predicted differentially expressed marker genes across the different clusters. A red box highlights the BVECs-I cluster. **(C', C'')** A list of brain-annotated genes was curated from the AmiGo annotation database and compared with the BVECs-I transcriptome. 63 genes were commonly expressed. Interestingly, several of these 63 genes were enriched within the BVECs-I cluster (**C''**; white boxed genes, **D**; enlarged circles).

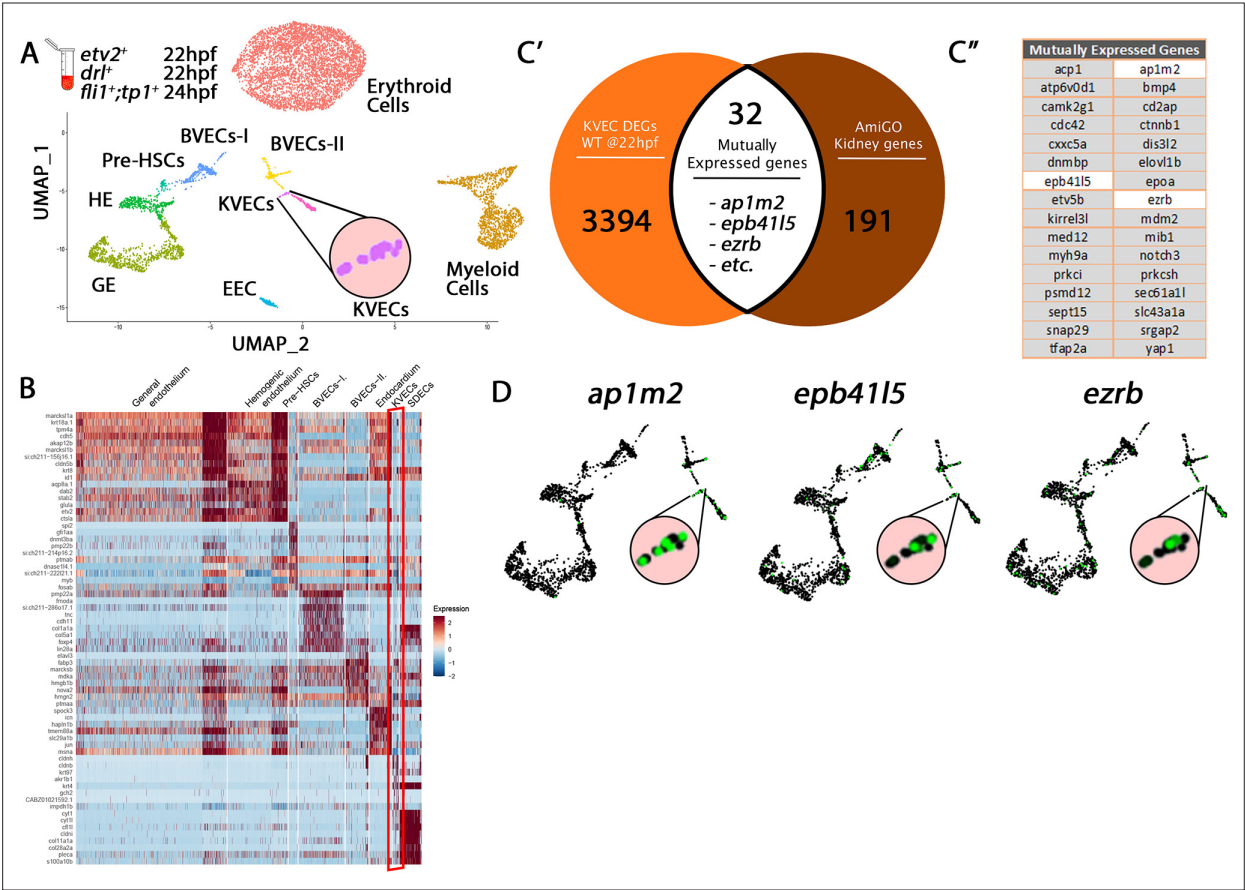


Figure 1—figure supplement 3. Comparison of KVEC Cluster genes to kidney annotated genes validates cluster origin. **(A)** Uniform manifold approximation (UMAP) plots of scRNA-seq data of total endothelial lineage cells collected from *TgBAC(etv2:Kaede)^{ci6}*, *Tg(fli1:DsRed)^{um13}*, *Tg(tp1:GFP)^{um14}*, and *Tg(drl:H2B-dendra)* embryos at 22–24 hpf. Clusters were named according to their gene expression: Erythroid, Lymphoid, General Endothelium (GE), Hemogenic Endothelium (HE), Pre-HSCs, Brain Vascular Endothelial Cells (BVECs-I and BVECs-II), Kidney Vascular Endothelial cells (KVECs), Endocardial Endothelial Cells (EECs), and somite-derived endothelial cells (SDECs). Color-coded marker gene expression levels are shown on corresponding clusters. A pink circle highlights the KVECs cluster. **(B)** Expression heatmap of 22–24 hpf single-cell transcriptome showing the top predicted differentially expressed marker genes across the different clusters. A red box highlights the KVECs cluster. **(C',C'')** A list of kidney-annotated genes was curated from the AmiGo annotation database and compared with the KVECs transcriptome. 32 genes were commonly expressed. Interestingly, several of these 32 genes were enriched within the KVECs cluster **(C''**; white boxed genes, **D**; enlarged circles).

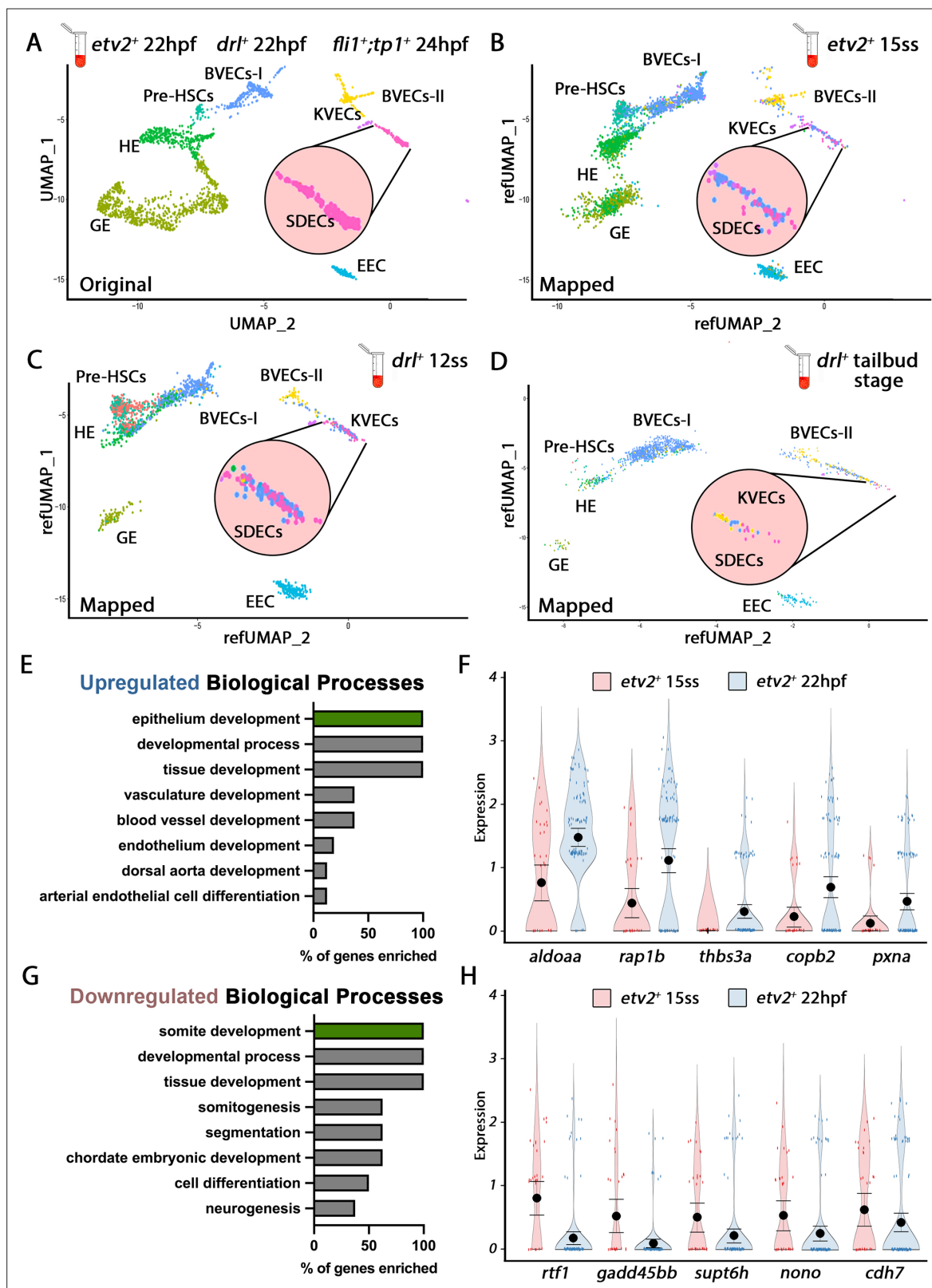


Figure 2. Cellular diversity within the vasculature can be traced back to the tailbud stage. (A) Uniform manifold approximation projection (UMAP) plots of scRNA-seq data of total endothelial lineage cells collected from *TgBAC(etv2:Kaede)^{c16}*, *Tg(fli1:DsRed)^{um13}*, *Tg(tp1:GFP)^{um14}*, and *Tg(drl:H2B-dendra)* embryos at 22–24 hpf. Clusters were named according to their gene expression: General Endothelium (GE), Hemogenic Endothelium (HE), Pre-HSCs, Brain Vascular Endothelial Cells (BVECs-I and BVECs-II), Kidney Vascular Endothelial cells (KVECs), Endocardial Endothelial Cells (EEC), and somite-

Figure 2 continued on next page

Figure 2 continued

derived endothelial cells (SDECs). Color-coded marker gene expression levels are shown on corresponding clusters. A pink circle highlights the SDEC cluster. **(B–D)** Referenced uniform manifold approximation projection (RefUMAP) plots of scRNA-seq data of total endothelial lineage cells collected from *etv2:Kaede*⁺ embryos at 15 ss **(B)** and *drl:H2B-dendra*⁺ embryos at 12 ss **(C)** and tailbud stage **(D)**. By cross-referencing the transcriptomes of EC subsets at each developmental stage to the 22–24 hpf ECs, we identified EC clusters with distinct transcriptomes as early as the tailbud stage. **(E–H)** Comparison of expression patterns of EC populations from early *TgBAC(etv2:Kaede)*^{ci6} 15 ss, and later 22 hpf *etv2:Kaede*⁺ in the 32 overlapping genes between the SDEC transcriptome data and the AmiGo somite annotated genes. **(E,F)** Representative genes that were upregulated in the *etv2:Kaede*⁺ 22 hpf samples compared to the 15 ss sample **(F)** and their suggested role in EC differentiation, according to GO biological processes **(E)**. **(G,H)** Representative genes that were downregulated in the *etv2:Kaede*⁺ 22 hpf samples compared to the 15 ss sample **(H)** and their suggested role in somitogenesis, according to GO biological processes **(G)**. The expression and downregulation of somitic genes within *etv2*⁺ ECs between 15 ss and 22 hpf highlight their somitic origin and loss of myogenic cell fate.

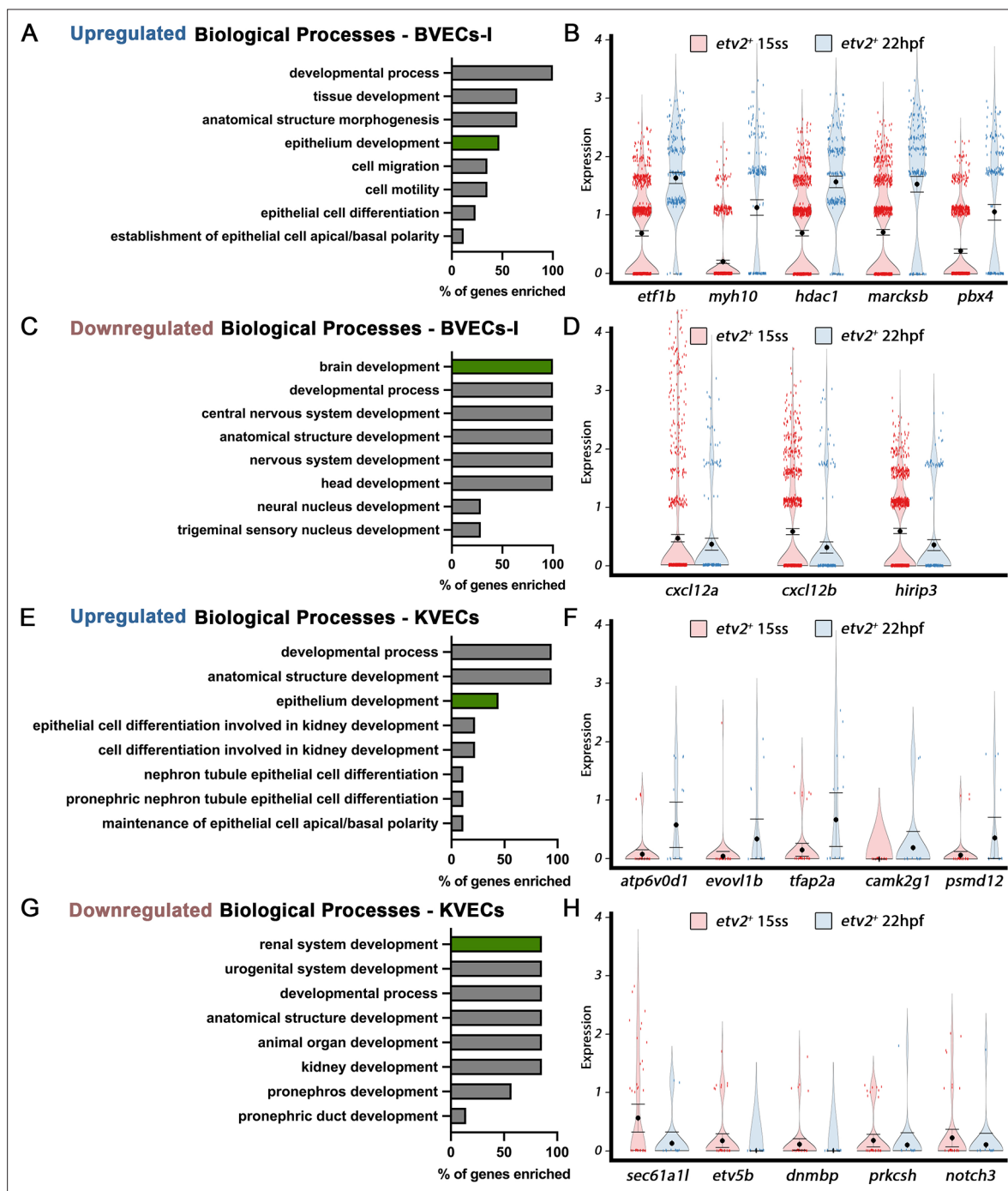


Figure 2—figure supplement 1. Differentially expressed genes between early and late ECs in BVECs-I or KVECs clusters highlight an early commitment to EC fate. (A–D) Comparison of expression patterns of EC populations from early *TgBAC(etv2:Kaede)^{c16}* 15 ss and later 22 hpf *etv2:Kaede⁺* ECs in the 63 overlapping genes between the BVECs-I transcriptome data and the AmiGo brain annotated genes. (A,B) Representative genes upregulated in the mixed vasculature 22 hpf samples compared to the 15 ss sample (B) and their suggested role in epithelium development, according to GO biological processes (A). (C,D) Representative genes downregulated in the mixed vasculature 22 hpf samples compared to the 15 ss sample (D) and their suggested role in brain development and neurogenesis, according to GO biological processes (C). (E–H) Comparison of expression patterns of EC populations from early *TgBAC(etv2:Kaede)^{c16}* 15 ss and later 22 hpf *etv2:Kaede⁺* ECs in the 32 overlapping genes between the KVECs transcriptome data and the AmiGo kidney annotated genes. (E,F) Representative genes upregulated in the mixed vasculature 22 hpf samples compared to the 15 ss sample (F) and their suggested role in epithelium development, according to GO biological processes (E). (G,H) Representative genes downregulated in the mixed vasculature 22 hpf samples compared to the 15 ss sample (H) and their suggested role in renal system development, according to GO biological processes (G).

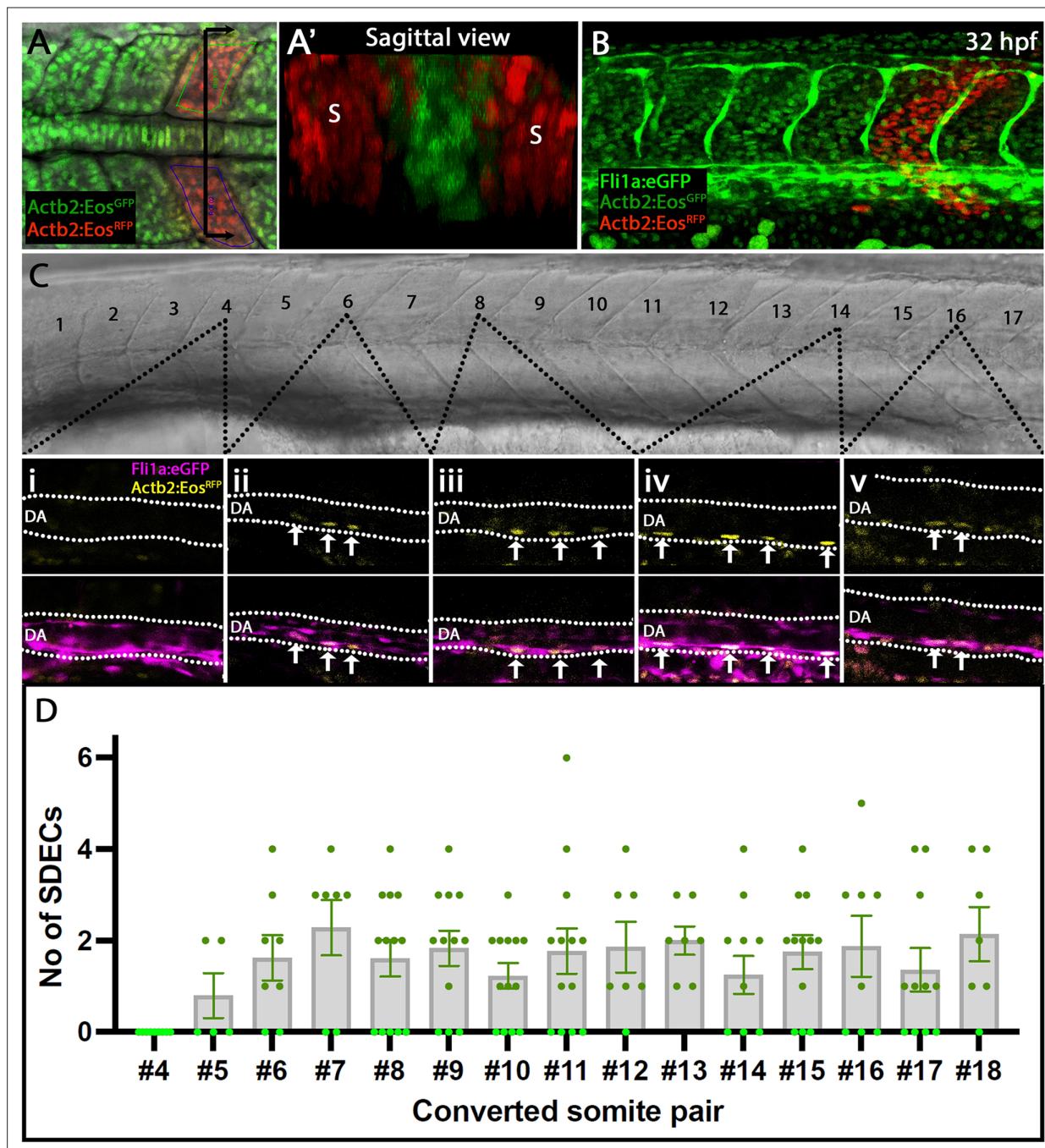


Figure 3. Rare SDECs emerge from trunk somites and migrate to the dorsal aorta. (A–D) *Tg(actb2:nls-Eos); Tg(fli1:eGFP)^{y1}* embryos were collected at developmental stages ranging from 4 to 18 ss. (A) Newly developed posterior somite pairs were selected by setting a region of interest and photoconverted by UV light. (A') A sagittal section through a pair of converted somite showing somite-specific conversion and lack of converted LPM-derived ECs. (B) At 32 hpf, embryos were laterally staged, and images of the dorsal aorta taken. SDECs were quantified in the dorsal aorta by examining individual z-stacks and visualizing colocalization of *fli1*⁺; *actb2:nlsEos^{RFP}* converted cells in *Tg(actb2:nls-Eos); Tg(fli1:eGFP)^{y1}* embryos (C–Cv). In *fli1:eGFP*⁺ embryos, we identified SDECs by observing *actb2:nlsEos^{RFP}* cells on the floor of the DA based on the brightfield channel. (D) We observed that trunk somites (numbers 5–18), located above the yolk tube extension, generated the most SDECs. Each somite pair contributed between 0–6 SDECs to the DA. s, somites; DA, dorsal aorta. In each converted somite pair, $n \geq 6$, with each point representing the SDEC count from one embryo. The median for each somite pair is indicated as a column, and the standard error of the mean (SEM) is indicated as an error bar.

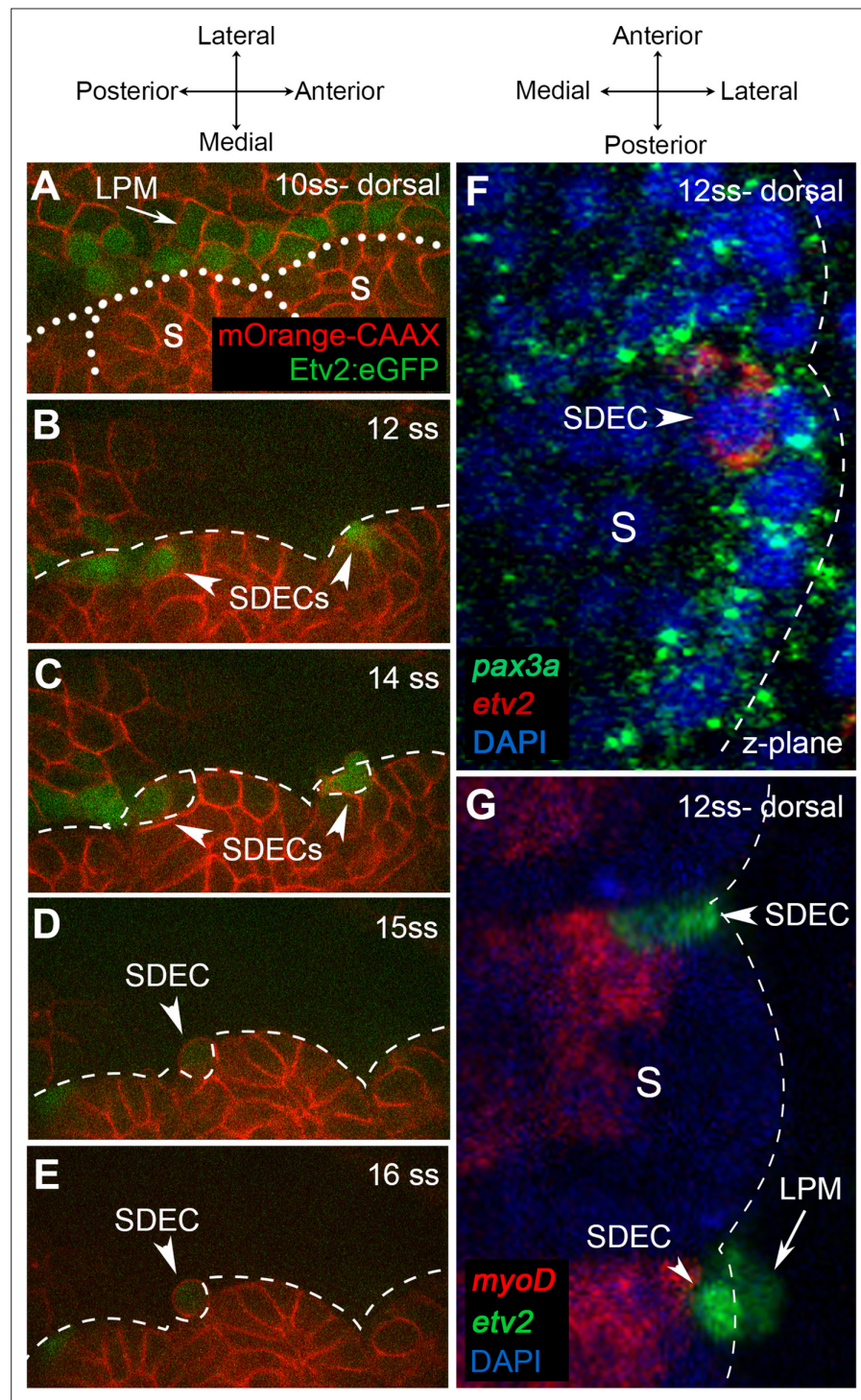


Figure 4. Endothelial cells emerge from the dermomyotome at 12 ss. **(A–E)** Time-lapse imaging from a dorsal view of *Tg(etv2.1:EGFP)^{tr372}* embryos injected with *mOrange:CAAX* mRNA and imaged between 10 ss and 15 ss. **(A)** The expression of *Etv2:GFP⁺* cells is visible along the LPM region (arrow) at 10 ss. At this stage, no *Etv2:GFP⁺* cells are visible in the somites. **(B)** Starting at 12 ss, the first *Etv2:GFP⁺* SDECs are detected in the lateral lip of the dermomyotome (arrowheads). Simultaneously, the LPM *Etv2:GFP⁺* cells start migrating to the midline. **(C)** Soon after emergence, SDECs change shape and become rounder (arrowheads). **(D–E)** *Etv2:GFP⁺* SDECs bud off from the somite as individual cells (arrowhead). **(F)** Dorsal view of a 12 ss embryo that was submitted to double fluorescent in situ hybridization for muscle progenitor marker *pax3a* (green) and endothelial marker *etv2* (red). *pax3a* expression reveals the dermomyotome compartment that contains muscle progenitor cells. An *etv2⁺* SDEC

Figure 4 continued on next page

Figure 4 continued

(red and arrowhead) is found in the dermomyotome, co-expressing *pax3a* (green), showing colocalization of an endothelial and muscle progenitor cell marker. We observed 1–2 *etv2*-positive cells per somite in each of the embryos examined (n=6). (**G**) Somitic *etv2*⁺ SDECs (green) do not co-express the muscle differentiation marker *myoD* (red), suggesting that *etv2* expression is restricted to the muscle progenitor region of the somite. Dashed white lines delimitate somite from the LPM (arrow). We observed 1–2 *etv2*-positive cells per somite in each of the embryos examined (n=6). s, somites; LPM, lateral plate mesoderm; SDECs, somite-derived endothelial cells.

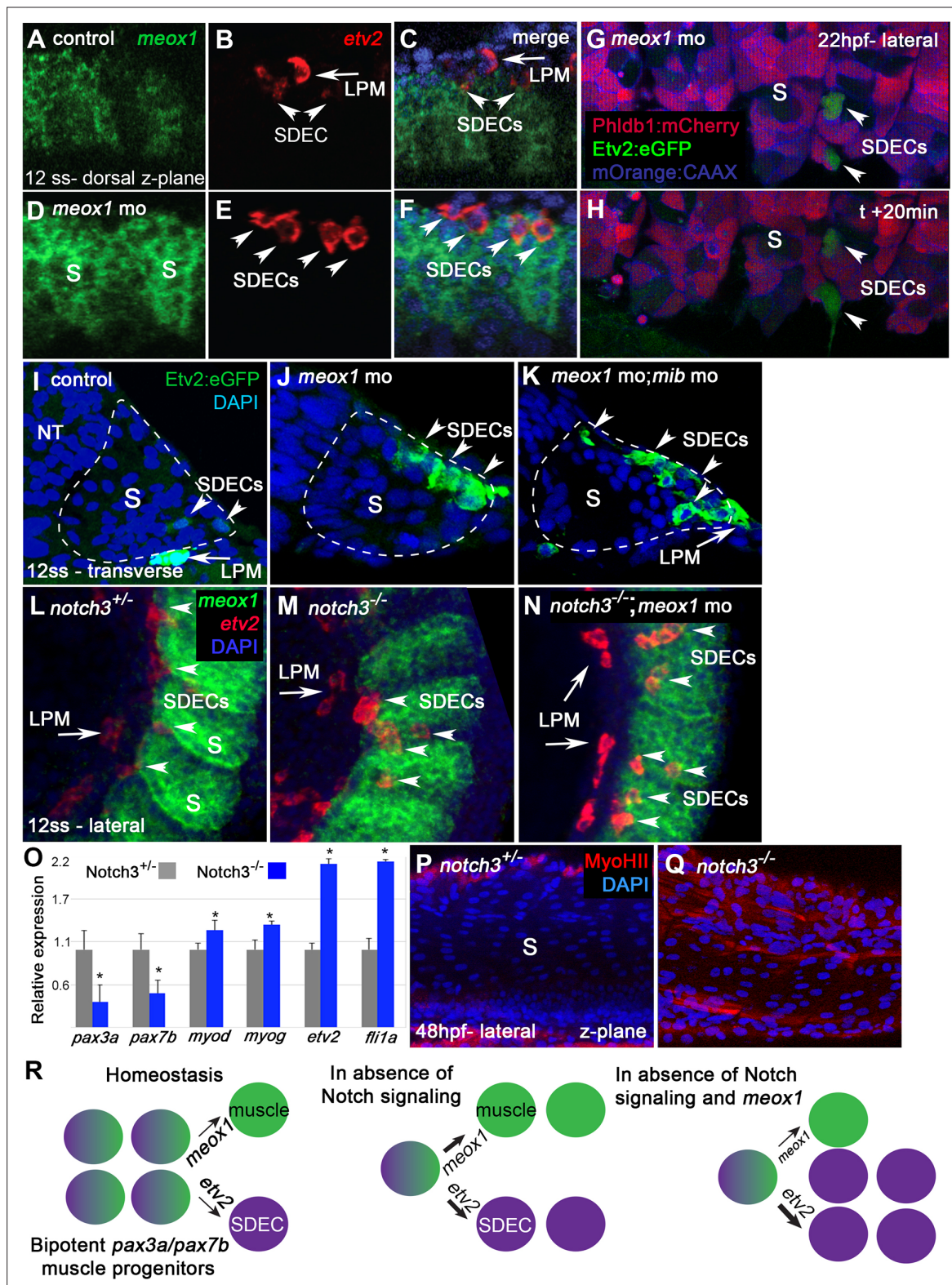


Figure 5. *notch* is required for the maintenance of a bipotent skeletal muscle progenitor population in the somite. (A–F) Dorsal view of 12 ss control (A–C) and *meox1* morphant embryos (D–F). Embryos were submitted to double fluorescent in situ hybridization for *meox1* (green) and *etv2* (red). In control and morphant embryos, *meox1*; *etv2* double-positive cells are detected within the somite compartment (arrowheads). (C,F) Overlay of *meox1* (green), *etv2* (red), and DAPI (blue). (D–F) Knockdown of *meox1* results in ectopic formation of double-positive cells within the somite (arrowheads). We observed 3–4 *etv2* positive cells per somite in the *meox1* morphants compared to 1–2 *etv2*-positive cells per somite in the siblings (n=3). (G–H) Time-

Figure 5 continued on next page

Figure 5 continued

lapse imaging of a 22 hpf *Tg(etv2.1:eGFP)^{z372}; Tg(phldb1:mCherry)* embryo, injected with *meox1* morpholino and *mOrange2:CAAX* mRNA to delineate cell boundaries. Knockdown of *meox1* results in an extension of the period that the dermomyotome can generate *Etv2:GFP⁺* cells (arrowheads). **(I–K)** Cross section of 12 ss *Tg(etv2.1:eGFP)^{z372}* embryo. In absence of *meox1* **(J)**, ectopic *Etv2:GFP⁺* cells are visible in epithelialized layer of the somites, compared to controls **(I)**. In embryos coinjected with *mib* and *meox1* morpholinos, the number of *Etv2:GFP⁺* cells within the somite compartment (dotted line) is substantially increased (arrowheads) **(K)**, suggesting that Notch signaling is dispensable for SDEC specification. **(L–N)** Lateral view of 12 ss embryos analyzed by FISH for *meox1* (green), *etv2* (red), and DAPI (blue). In *notch3^{+/−}* heterozygote controls **(L)** and *notch3^{−/−}* mutant embryos **(M)**, *etv2⁺* SDECs are detected in the somites. **(N)** *notch3^{−/−}* mutant embryos co-injected with *meox1* morpholino results in ectopic formation of *etv2; meox1* double positive cells (arrowheads). We observed 2–4 *etv2*-positive cells per somite in the *notch3* mutants and >6 *etv2*-positive cells in the *notch3* mutants; *Mib* morphants (n=3). **(O)** qRT-PCR in 24 hpf *notch3^{−/−}* mutant embryos and sibling controls. Genetic ablation of *notch3* results in decreased expression of muscle progenitor markers *pax3a* and *pax7b*; increased expression of muscle differentiation genes, *myod* and *myog*, and endothelial markers, *etv2*, and *fli1*. Asterisks denote a statistically significant difference (p<0.05, unpaired, two-tailed Student's t-test; n=3.) **(P,Q)** *notch3^{−/−}* mutant embryos show premature expression of MyoHIII in 48 hpf embryos **(Q)** compared to sibling controls **(P)**. **(R)** Summary cartoon for the role of Notch signaling in the maintenance of bipotent-muscle progenitors (bipotent muscle progenitors in purple and green; muscle cells in green; SDECs in purple). s, somites; LPM, lateral plate mesoderm; SDECs, somite-derived endothelial cells.

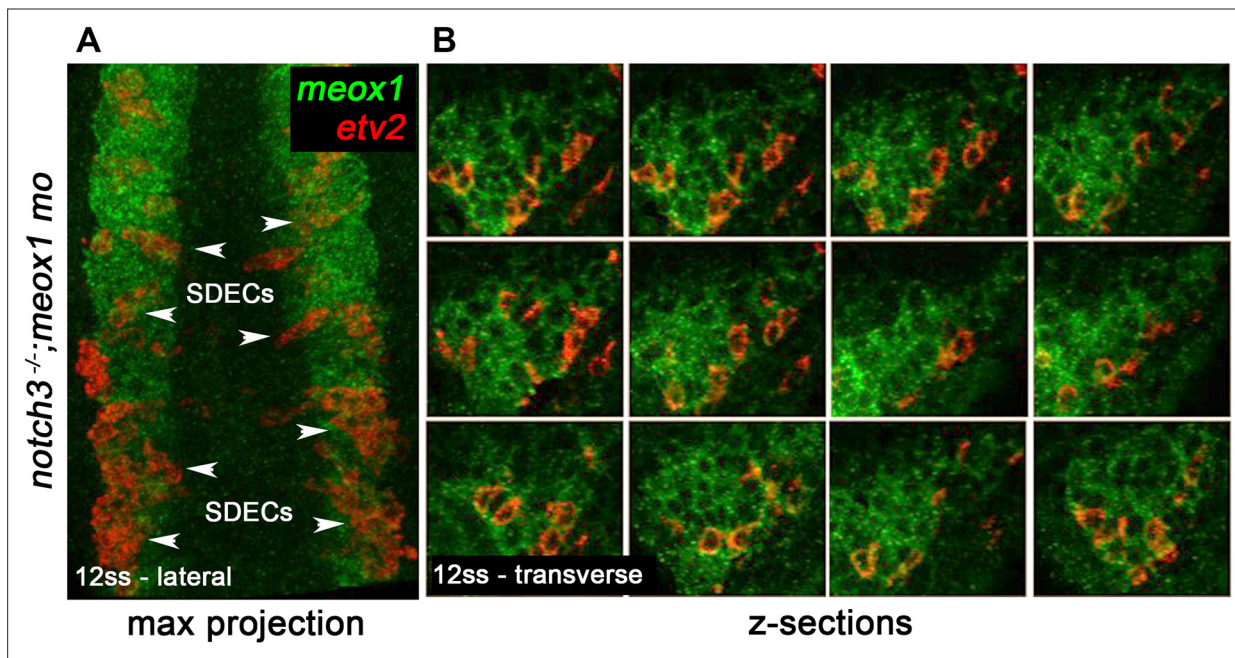


Figure 5—figure supplement 1. Bipotent muscle progenitor cells contain endothelial potential that can reach the dermomyotome compartment. **(A)** Max projection of 12 hpf *notch3*^{-/-} mutant embryos injected with *meox1* morpholino shows broad endothelial potential within the somite compartment by the ectopic formation of double positive *meox1* (green) and *etv2* (red) SDECs (arrowheads). **(B)** Z-sections of a representative dermomyotome compartment show the extent of double-positive cells. SDECs, somite-derived endothelial cells.

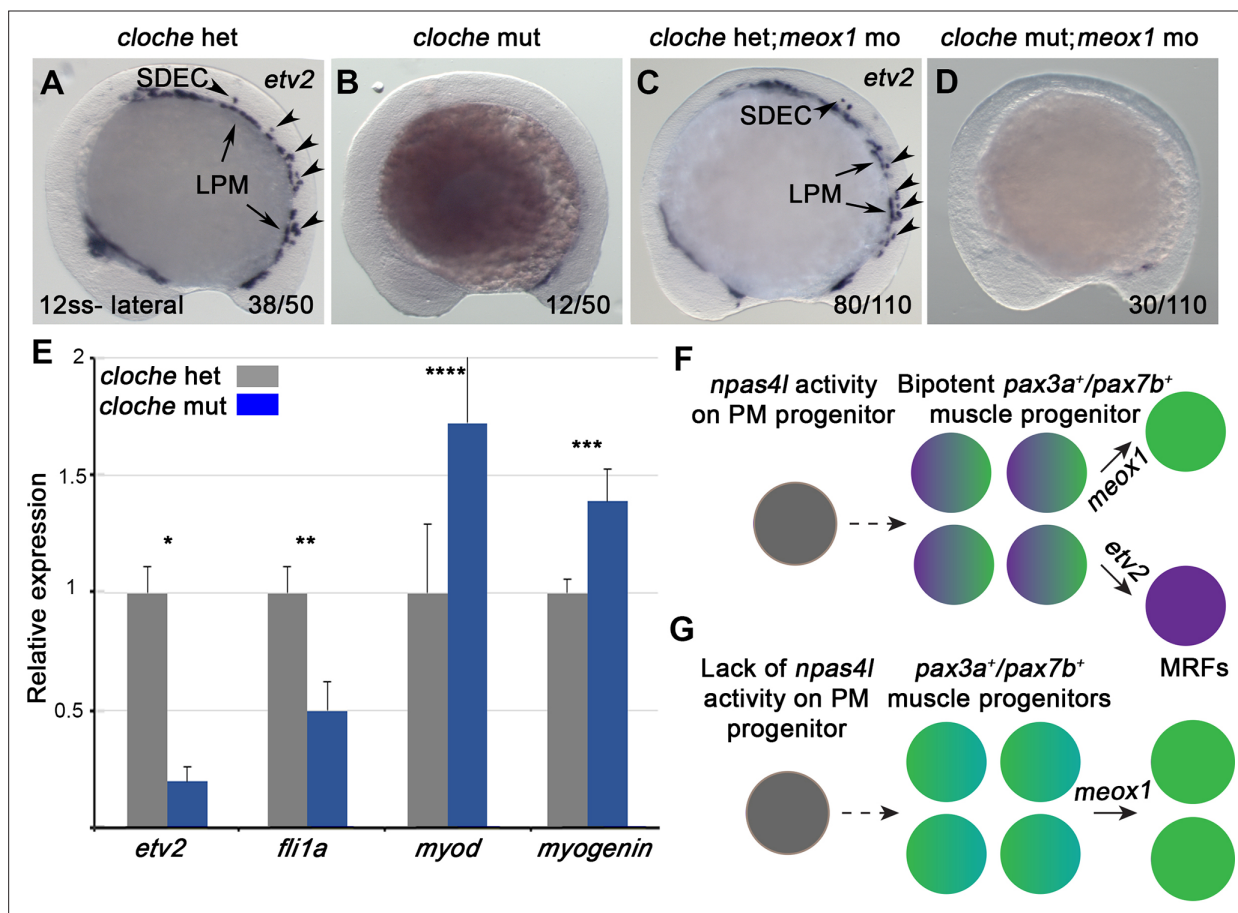


Figure 6. *npas4l* is required for the specification of SDECs. (A–D) WISH for *etv2* in 12 ss *npas4l*^{-/-} (*cloche*) mutant and control embryos. (B) *cloche* mutant embryos show an absence of *etv2* expression along the A-P axis of the embryo, compared to sibling control (A). (D) Similarly, *cloche* mutant embryos injected with *meox1* morpholino show loss of *etv2* expression, compared to sibling control (C). (E) qRT-PCR of *cloche* mutant embryos shows expected loss of endothelial genes (*fli1* and *etv2*) and concomitant increase of muscle differentiation genes (*myod* and *myog*), compared to sibling control. All genes analyzed between *cloche* mutant and *cloche* het embryos showed a statistically significant difference ($p < 0.001$, unpaired, two-tailed Student's t-test; $n = 3$). (F, G) Summary cartoon for the effect of *npas4l* on endothelial cell competence in PM progenitors (early mesoderm progenitor in grey; bipotent muscle progenitor in purple and green; muscle cells in green; endothelial cells in purple). LPM, lateral plate mesoderm; SDECs, somite-derived endothelial cells.

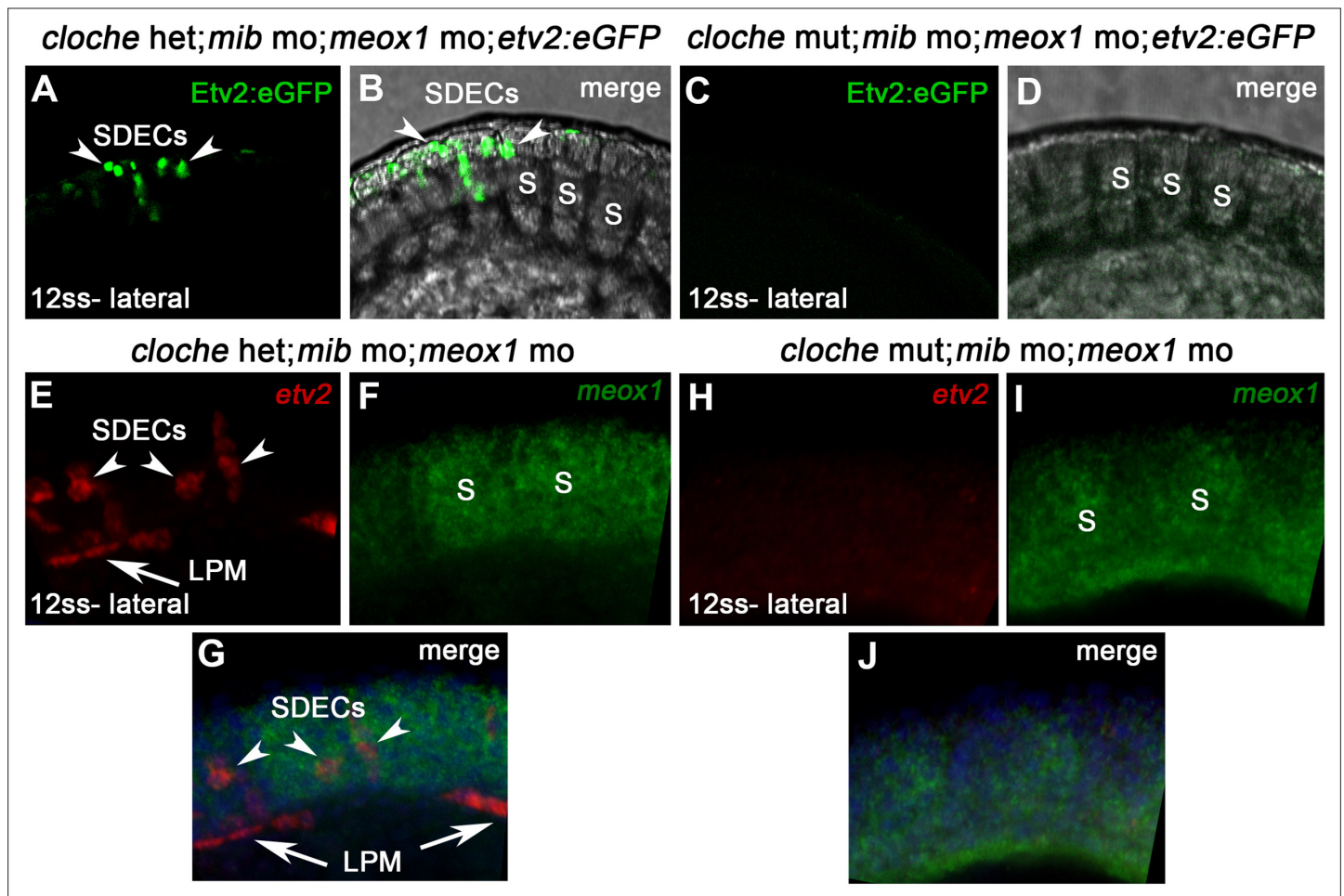


Figure 6—figure supplement 1. *npas4l* is required for the specification of SDECs. (A–D) *Tg(etv2.1:eGFP)^{z1372}*; *cloche* mutant and heterozygous embryos were injected with *meox1* and *mib* morpholinos. (C,D) *Cloche* mutant embryos showed loss of *Etv2:eGFP* expression in the LPM and somites at 12 ss compared with control embryos (A,B; arrowheads). (E–J) *Cloche* mutant and heterozygous embryos were injected with both *meox1* and *mib* morpholinos. FISH for *meox1* (green) and *etv2* (red) shows loss of all *etv2* and *meox1* double-positive cells in *cloche* mutants (H–J) compared with control embryos (E–G; arrowheads) at 12 ss. S, somites; LPM, lateral plate mesoderm; SDECs, somite-derived endothelial cells.

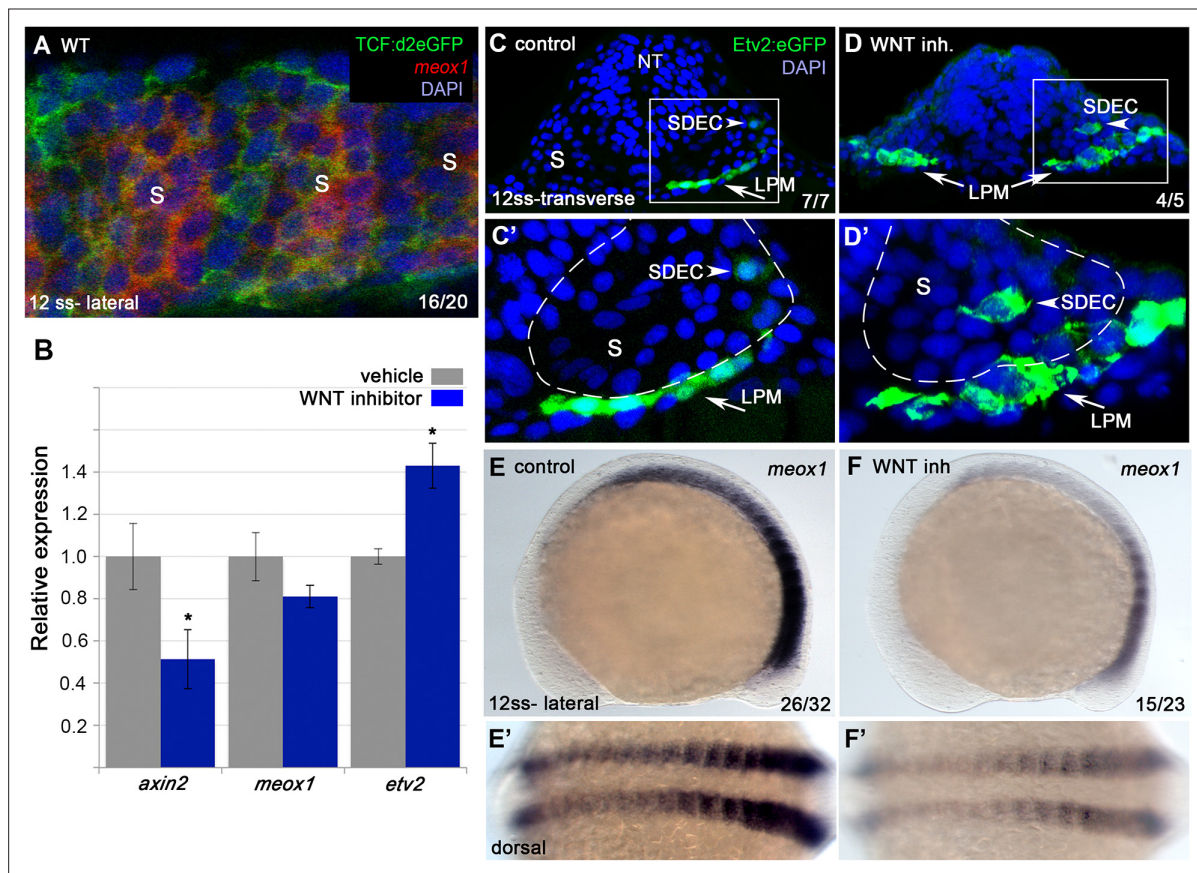


Figure 7. Wnt signaling is required for the regionalization of SDECs. (A) FISH for *meox1* (red) and antibody staining for a destabilized Wnt/TCF reporter line (green) show co-expression of GFP and *meox1* within the somite. (B) Inhibition of Wnt signaling using the chemical inhibitor IWP2 from 2 ss to 15 ss results in decreased expression of *axin2* and *meox1* with a concomitant increase of the expression of *etv2* by qRT-PCR. We observed a reduction in *meox1* expression, although not statistically significant. All genes analyzed between Wnt inhibitor and control embryos, except *meox1*, showed a statistically significant difference ($p < 0.001$, unpaired, two-tailed Student's t-test; $n = 3$.) (C–D') Cross section of *Tg(etv2.1:EGFP)⁴³⁷²* embryos treated with IWP2 from 2 ss to 15 ss. *wnt* inhibition results in ectopic formation of *Etv2:GFP⁺* cells within the somite (arrowheads). (C',D') enlargement of somite compartment (dashed lines). Notice LPM cells migrating under the sclerotome (arrows). (E–F') IWP2 control and treated embryos. *wnt* inhibition results in decreased expression of *meox1* by WISH, compared to control embryos. (E,F) Lateral view. (E',F') Dorsal view. s, somites; LPM, lateral plate mesoderm; SDECs, somite-derived endothelial cells.

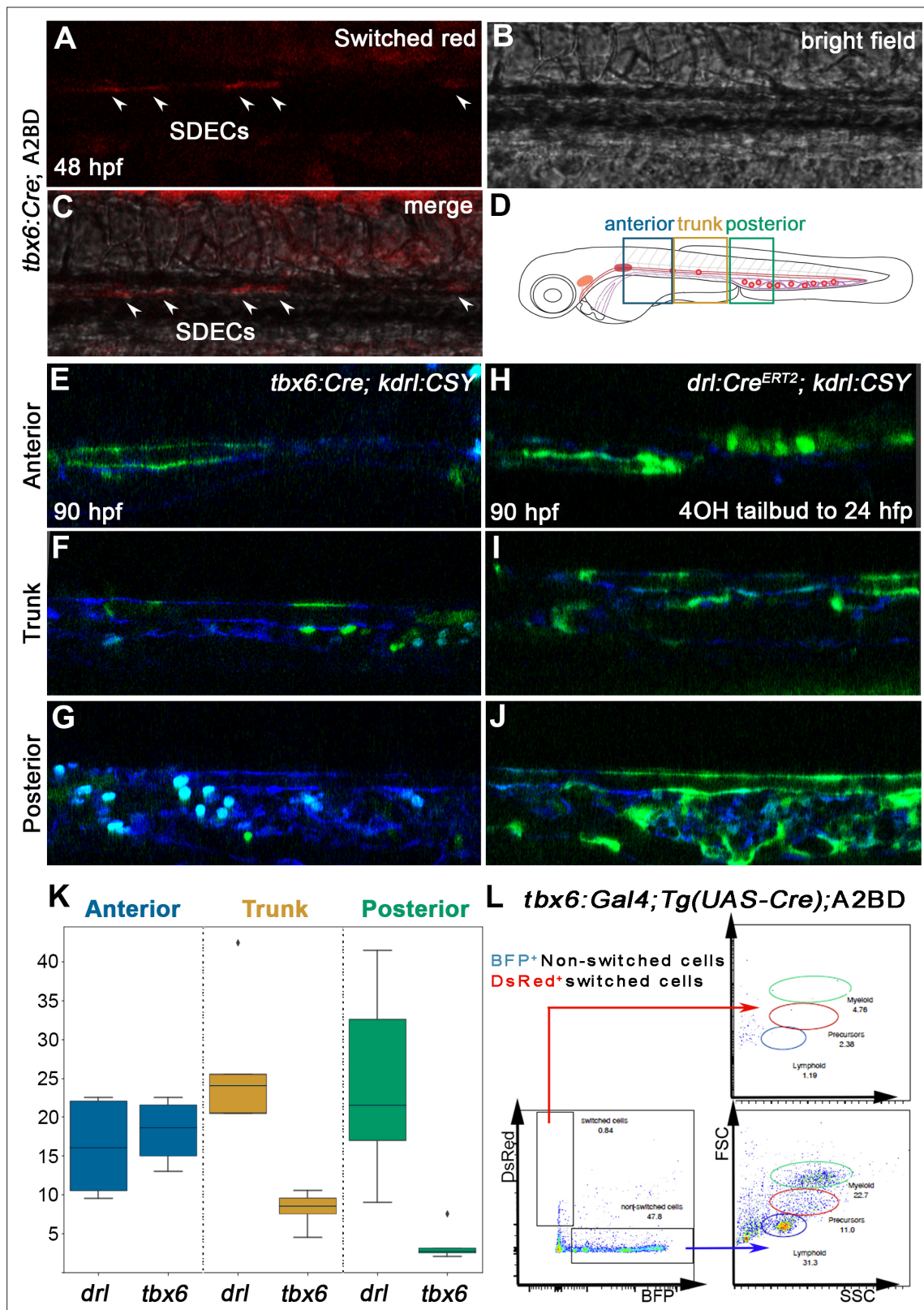


Figure 8. SDECs contribute to the dorsal aorta but do not generate HSPCs. (A–C) Lineage tracing of SDECs using *tbx6:Gal4; Tg(UAS-Cre); A2BD* shows *dsRed*⁺ cells in the vasculature region at 48 hpf (arrowheads). (E–J) Using a vasculature-specific switch line *Tg(BACkdrl:LOXP-AmCyan-LOXP-ZsYellow* (referred to as *kdrl:CSY*), we observe the contribution of SDECs or LPM-derived endothelial cells to the vasculature. (E–G) For SDEC labeling, a PM-specific driver *tbx6:Gal4; Tg(UAS-Cre)* was used. PM-derived YFP⁺ SDECs are observed in the vasculature of imaged embryos. (H–J) For LPM-specific

Figure 8 continued on next page

Figure 8 continued

EC labeling, a *Tg(drl:Cre^{ERT2})* was used and treated with 10 μ m tamoxifen starting at 8 hpf. YFP⁺ ECs are observed in all regions of the vasculature. **(K)** Quantification of YFP⁺ SDECs and ECs from *tbx6* or *drl* switched embryos, respectively. Quantifications were based on independent experiments per transgenic background with n=23 for *tbx6* switched embryos and n=9 for *drl* switch embryos. **(L)** Analysis of the adult kidney marrow of *tbx6:Gal4; Tg(UAS-Cre); A2BD* animals shows no contribution to hematopoietic cells from switched DsRed⁺ SDECs through flow cytometry analysis, whereas the FSC/SSC distribution of the unswitched BFP⁺ ECs corresponds to all blood lineages (quantifications based from independent experiments with a total of n=21 samples). SDECs, somite-derived endothelial cells.

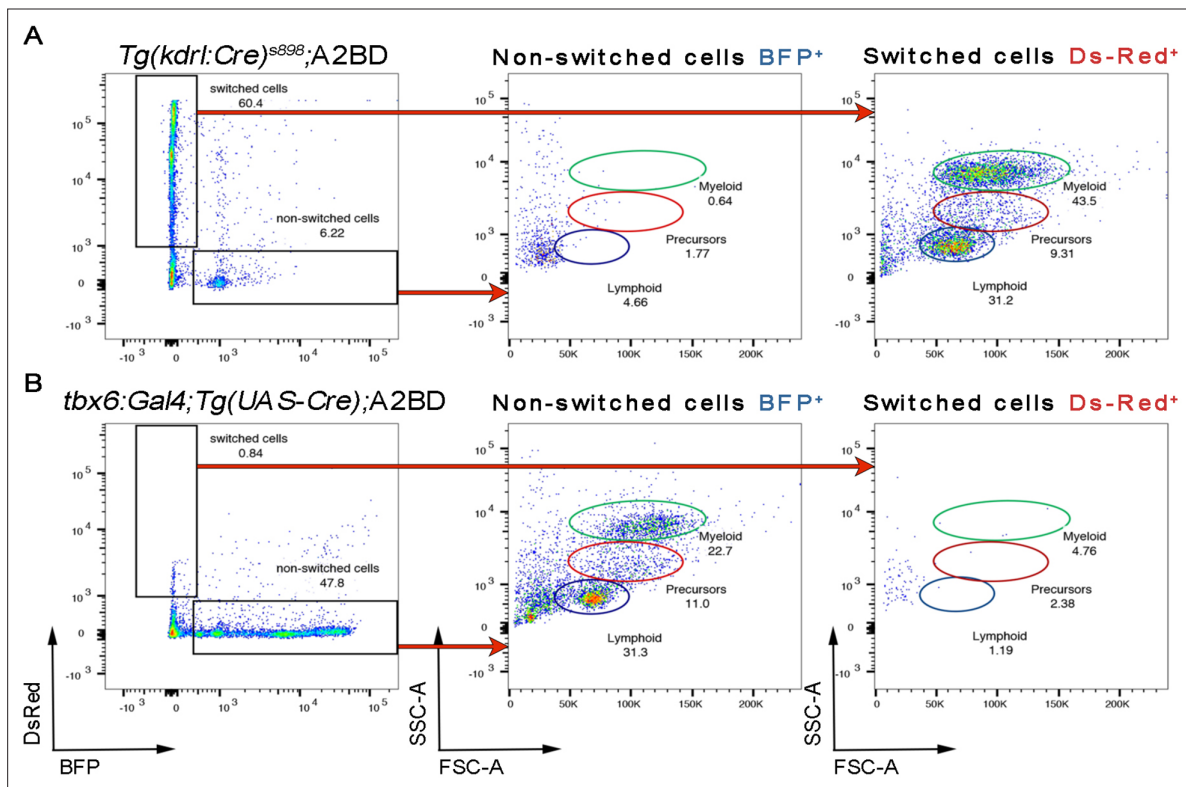


Figure 8—figure supplement 1. Paraxial mesoderm does not generate HSPCs. (A) *kdr1:Cre; A2BD* and (B) *tbx6:Gal4; Tg(UAS-Cre); A2BD* adult kidney marrow was analyzed by flow cytometry. Top row illustrates that the hematopoietic lineages of *kdr1:Cre; A2BD* originate from switched DsRed⁺ ECs (A), whereas in the *tbx6:Gal4; Tg(UAS-Cre); A2BD*, BFP⁺ non-switched ECs are the source of the hematopoietic system. DsRED⁺ SDECs do not give rise to hematopoietic lineages (B).

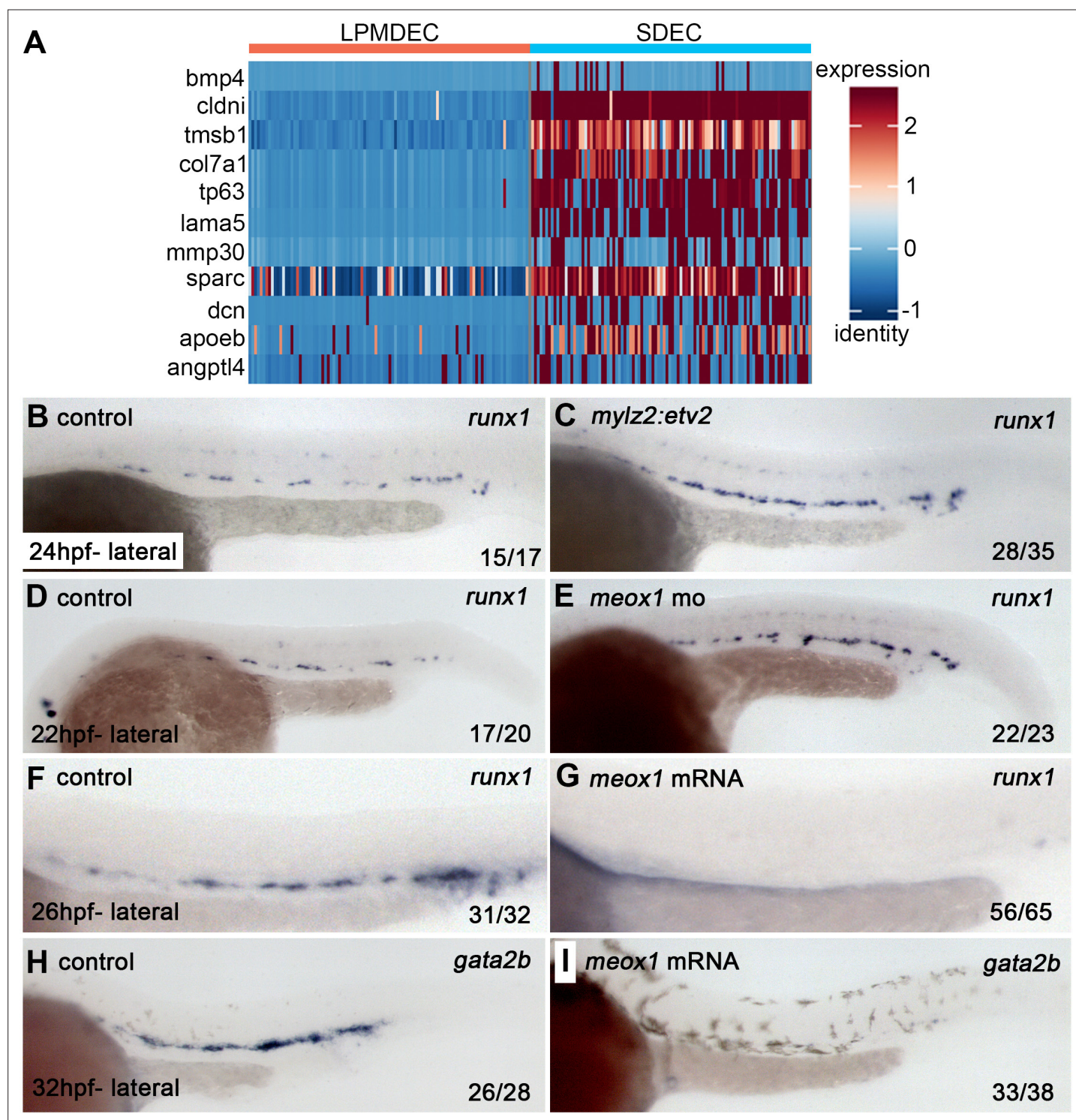


Figure 9. SDECs act as a vascular niche for hemogenic endothelium. **(A)** Heatmap of genes differentially regulated between LPM-derived endothelial cells (LPMDEC sample is composed of pre-HSCs and HE clusters) and SDECs. **(B,C)** Zebrafish embryos were injected with an expression vector containing a somite-specific promoter, *mylz2*, driving an *etv2* transgene to ectopically induced SDECs. By WISH, an increase in *runx1* expression was observed at 24 hpf compared to embryos injected with an empty *mylz2* vector. **(D,E)** Similarly, *meox1* morphants exhibit an increased expression of *runx1* by WISH compared to uninjected control embryos. **(F–I)** Conversely, overexpression of *meox1* by mRNA injection strongly reduces the hemogenic markers *runx1* and *gata2b*. SDECs, somite-derived endothelial cells.